

World Journal of *Clinical Cases*

World J Clin Cases 2021 March 16; 9(8): 1761-2021



REVIEW

- 1761 Cardiac rehabilitation and its essential role in the secondary prevention of cardiovascular diseases
Winnige P, Vysoky R, Dosbaba F, Batalik L

ORIGINAL ARTICLE**Case Control Study**

- 1785 Association between homeobox protein transcript antisense intergenic ribonucleic acid genetic polymorphisms and cholangiocarcinoma
Lampropoulou DI, Laschos K, Aravantinos G, Georgiou K, Papiris K, Theodoropoulos G, Gazouli M, Filippou D

Retrospective Study

- 1793 Risk factors for post-hepatectomy liver failure in 80 patients
Xing Y, Liu ZR, Yu W, Zhang HY, Song MM

- 1803 Outcomes of laparoscopic bile duct exploration for choledocholithiasis with small common bile duct
Huang XX, Wu JY, Bai YN, Wu JY, Lv JH, Chen WZ, Huang LM, Huang RF, Yan ML

Observational Study

- 1814 Three-dimensional finite element analysis with different internal fixation methods through the anterior approach
Xie XJ, Cao SL, Tong K, Zhong ZY, Wang G
- 1827 Bedside cardiopulmonary ultrasonography evaluates lung water content in very low-weight preterm neonates with patent ductus arteriosus
Yu LF, Xu CK, Zhao M, Niu L, Huang XM, Zhang ZQ

CASE REPORT

- 1835 Conservative endodontic management using a calcium silicate bioceramic sealer for delayed root fracture: A case report and review of the literature
Zheng P, Shen ZY, Fu BP
- 1844 Brain magnetic resonance imaging findings and radiologic review of maple syrup urine disease: Report of three cases
Li Y, Liu X, Duan CF, Song XF, Zhuang XH
- 1853 A three-year clinical investigation of a Chinese child with craniometaphyseal dysplasia caused by a mutated ANKH gene
Wu JL, Li XL, Chen SM, Lan XP, Chen JJ, Li XY, Wang W
- 1863 Intradural osteomas: Report of two cases
Li L, Ying GY, Tang YJ, Wu H

- 1871** Gastroesophageal varices in a patient presenting with essential thrombocythemia: A case report
Wang JB, Gao Y, Liu JW, Dai MG, Yang SW, Ye B
- 1877** Chest pain showing precordial ST-segment elevation in a 96-year-old woman with right coronary artery occlusion: A case report
Wu HY, Cheng G, Cao YW
- 1885** Subcutaneous panniculitis-like T-cell lymphoma invading central nervous system in long-term clinical remission with lenalidomide: A case report
Sun J, Ma XS, Qu LM, Song XS
- 1893** Imaging findings of primary pulmonary synovial sarcoma with secondary distant metastases: A case report
Li R, Teng X, Han WH, Li Y, Liu QW
- 1901** Severe community-acquired pneumonia caused by *Leptospira interrogans*: A case report and review of literature
Bao QH, Yu L, Ding JJ, Chen YJ, Wang JW, Pang JM, Jin Q
- 1909** Bilateral common peroneal neuropathy due to rapid and marked weight loss after biliary surgery: A case report
Oh MW, Gu MS, Kong HH
- 1916** Retroperitoneal laparoscopic partial resection of the renal pelvis for urothelial carcinoma: A case report
Wang YL, Zhang HL, Du H, Wang W, Gao HF, Yu GH, Ren Y
- 1923** 17 α -hydroxylase/17,20 carbon chain lyase deficiency caused by p.Tyr329fs homozygous mutation: Three case reports
Zhang D, Sun JR, Xu J, Xing Y, Zheng M, Ye SD, Zhu J
- 1931** Epithelioid angiomyolipoma of the pancreas: A case report and review of the literature
Zhu QQ, Niu ZF, Yu FD, Wu Y, Wang GB
- 1940** Computed tomography imaging features for amyloid dacryolith in the nasolacrimal excretory system: A case report
Che ZG, Ni T, Wang ZC, Wang DW
- 1946** Epidural analgesia followed by epidural hydroxyethyl starch prevented post-dural puncture headache: Twenty case reports and a review of the literature
Song LL, Zhou Y, Geng ZY
- 1953** Extracorporeal membrane oxygenation for coronavirus disease 2019-associated acute respiratory distress syndrome: Report of two cases and review of the literature
Wen JL, Sun QZ, Cheng Z, Liao XZ, Wang LQ, Yuan Y, Li JW, Hou LS, Gao WJ, Wang WJ, Soh WY, Li BF, Ma DQ
- 1968** Human parvovirus B19-associated early postoperative acquired pure red cell aplasia in simultaneous pancreas-kidney transplantation: A case report
Wang H, Fu YX, Song WL, Wang Z, Feng G, Zhao J, Nian YQ, Cao Y

- 1976** Diabetes insipidus with impaired vision caused by germinoma and perioptic meningeal seeding: A case report
Yang N, Zhu HJ, Yao Y, He LY, Li YX, You H, Zhang HB
- 1983** Madelung disease: A case report
Chen KK, Ni LS, Yu WH
- 1989** Laryngopharyngeal reflux disease management for recurrent laryngeal contact granuloma: A case report
Li K, Chen WY, Li YY, Wang TL, Tan MJ, Chen Z, Chen H
- 1996** *Mycobacterium abscessus* infection after facial injection of argireline: A case report
Chen CF, Liu J, Wang SS, Yao YF, Yu B, Hu XP
- 2001** Inadvertent globe penetration during retrobulbar anesthesia: A case report
Dai Y, Sun T, Gong JF
- 2008** Systemic lupus erythematosus combined with primary hyperfibrinolysis and protein C and protein S deficiency: A case report
Liao YX, Guo YF, Wang YX, Liu AH, Zhang CL
- 2015** Interstitial lung disease induced by the roots of *Achyranthes japonica* Nakai: Three case reports
Moon DS, Yoon SH, Lee SI, Park SG, Na YS

ABOUT COVER

Gokul Sridharan, MD, PhD, Associate Professor, Oral Pathology and Microbiology, YMT Dental College and Hospital, Navi Mumbai, Mumbai 400018, Maharashtra, India. drgokuls@gmail.com

AIMS AND SCOPE

The primary aim of *World Journal of Clinical Cases* (WJCC, *World J Clin Cases*) is to provide scholars and readers from various fields of clinical medicine with a platform to publish high-quality clinical research articles and communicate their research findings online.

WJCC mainly publishes articles reporting research results and findings obtained in the field of clinical medicine and covering a wide range of topics, including case control studies, retrospective cohort studies, retrospective studies, clinical trials studies, observational studies, prospective studies, randomized controlled trials, randomized clinical trials, systematic reviews, meta-analysis, and case reports.

INDEXING/ABSTRACTING

The WJCC is now indexed in Science Citation Index Expanded (also known as SciSearch®), Journal Citation Reports/Science Edition, Scopus, PubMed, and PubMed Central. The 2020 Edition of Journal Citation Reports® cites the 2019 impact factor (IF) for WJCC as 1.013; IF without journal self cites: 0.991; Ranking: 120 among 165 journals in medicine, general and internal; and Quartile category: Q3. The WJCC's CiteScore for 2019 is 0.3 and Scopus CiteScore rank 2019: General Medicine is 394/529.

RESPONSIBLE EDITORS FOR THIS ISSUE

Production Editor: Jia-Hui Li; Production Department Director: Yu-Jie Ma; Editorial Office Director: Jin-Li Wang.

NAME OF JOURNAL

World Journal of Clinical Cases

ISSN

ISSN 2307-8960 (online)

LAUNCH DATE

April 16, 2013

FREQUENCY

Thrice Monthly

EDITORS-IN-CHIEF

Dennis A Bloomfield, Sandro Vento, Bao-Gan Peng

EDITORIAL BOARD MEMBERS

<https://www.wjgnet.com/2307-8960/editorialboard.htm>

PUBLICATION DATE

March 16, 2021

COPYRIGHT

© 2021 Baishideng Publishing Group Inc

INSTRUCTIONS TO AUTHORS

<https://www.wjgnet.com/bpg/gerinfo/204>

GUIDELINES FOR ETHICS DOCUMENTS

<https://www.wjgnet.com/bpg/GerInfo/287>

GUIDELINES FOR NON-NATIVE SPEAKERS OF ENGLISH

<https://www.wjgnet.com/bpg/gerinfo/240>

PUBLICATION ETHICS

<https://www.wjgnet.com/bpg/GerInfo/288>

PUBLICATION MISCONDUCT

<https://www.wjgnet.com/bpg/gerinfo/208>

ARTICLE PROCESSING CHARGE

<https://www.wjgnet.com/bpg/gerinfo/242>

STEPS FOR SUBMITTING MANUSCRIPTS

<https://www.wjgnet.com/bpg/GerInfo/239>

ONLINE SUBMISSION

<https://www.f6publishing.com>

Observational Study

Three-dimensional finite element analysis with different internal fixation methods through the anterior approach

Xian-Jin Xie, Sheng-Lu Cao, Kai Tong, Zi-Yi Zhong, Gang Wang

ORCID number: Xian-Jin Xie 0000-0001-5760-5973; Sheng-Lu Cao 0000-0002-6172-7575; Kai Tong 0000-0002-7248-0248; Zi-Yi Zhong 0000-0001-8151-4836; Gang Wang 0000-0002-4432-1901.

Author contributions: Xie XJ conceived and coordinated the study, designed, performed, and analyzed the experiments, and wrote the paper; Cao SL, Tong K, Zhong ZY, and Wang G carried out the data collection, data analysis, and revised the paper; All authors reviewed the results and approved the final version of the manuscript.

Supported by National Natural Science Foundation of China, No. 81272008.

Institutional review board statement: The study was approved by the ethics committee of Nanfang Hospital, Southern Medical University.

Informed consent statement: All study participants provided informed written consent prior to study enrollment.

Conflict-of-interest statement: There are no conflicts of interest to report.

Data sharing statement: No additional data are available.

Xian-Jin Xie, Sheng-Lu Cao, Zi-Yi Zhong, Gang Wang, Department of Orthopaedic Surgery, Nanfang Hospital, Southern Medical University, Guangzhou 510515, Guangdong Province, China

Kai Tong, Department of Orthopaedic Surgery, Zhongnan Hospital, Wuhan University, Wuhan 430000, Hubei Province, China

Corresponding author: Gang Wang, MD, Doctor, Department of Orthopaedic Surgery, Nanfang Hospital, Southern Medical University, No. 1838 Guangzhou Avenue North, Baiyun District, Guangzhou 510515, Guangdong Province, China. 664032160@qq.com

Abstract

BACKGROUND

With the modernization of society and transportation in the last decades in China, the incidence of high-energy trauma increased sharply in China, including that of acetabular fractures.

AIM

To establish different finite element models for acetabular posterior column fractures involving the quadrilateral area of the acetabulum.

METHODS

The three-dimensional models of the normal and fractured pelvis and the five internal fixations were established using the computed tomography data of the pelvis of a living volunteer. After the vertebral body model was inserted in the way of origin matching and all cancellous bones were copied using the duplicated cancellous bone model as the subtractive entity, the Boolean operation was performed on the pelvis model to obtain the model of the complete pelvis cortical and cancellous bones.

RESULTS

In the standing position, the maximum stress was 46.21 MPa. In the sitting position, the sacrum bore the simulated gravity load at the upper end. When comparing the five fixations, there were no significant differences in the stress mean values among groups (sitting: $P = 0.9794$; standing: $P = 0.9741$). In terms of displacement, the average displacement of the internal iliac plate group was smaller than that of the spring plate group ($P = 0.002$), and no differences were observed between the other pairs of groups (all $P > 0.05$). In the standing position,

STROBE statement: The authors have read the STROBE Statement – checklist of items, and the manuscript was prepared and revised according to the STROBE Statement – checklist of items.

Open-Access: This article is an open-access article that was selected by an in-house editor and fully peer-reviewed by external reviewers. It is distributed in accordance with the Creative Commons Attribution NonCommercial (CC BY-NC 4.0) license, which permits others to distribute, remix, adapt, build upon this work non-commercially, and license their derivative works on different terms, provided the original work is properly cited and the use is non-commercial. See: <http://creativecommons.org/licenses/by-nc/4.0/>

Manuscript source: Unsolicited manuscript

Specialty type: Medicine, research and experimental

Country/Territory of origin: China

Peer-review report's scientific quality classification

Grade A (Excellent): 0
Grade B (Very good): B
Grade C (Good): C
Grade D (Fair): 0
Grade E (Poor): 0

Received: September 24, 2020

Peer-review started: September 24, 2020

First decision: December 14, 2020

Revised: January 6, 2021

Accepted: January 25, 2021

Article in press: January 25, 2021

Published online: March 16, 2021

P-Reviewer: Corrales FJ, Shimizu Y

S-Editor: Zhang L

L-Editor: Filipodia

P-Editor: Wang LL



there were no significant differences in the mean value of displacement among the groups ($P = 0.2985$). It can be seen from the stress nephogram of the internal fixations in different positions that the stress of the internal fixation was mainly concentrated in the fracture segment.

CONCLUSION

There were no significant differences among the fixations for acetabular posterior column fractures involving the quadrilateral area of the acetabulum.

Key Words: Acetabulum; Hip fractures; Analysis; Finite element; Fracture fixation; Orthopedic fixation devices

©The Author(s) 2021. Published by Baishideng Publishing Group Inc. All rights reserved.

Core Tip: Acetabular fractures are challenging, especially fractures of the quadrilateral area. Obtaining a three-dimensional finite element model of the pelvis is an effective method for biomechanical research and can provide some basis for the biomechanical characteristics of different fixation methods. This study aimed to establish different finite element models (in simulated standing and sitting positions) of the internal iliac plate, combined plate of anterior and posterior columns, triangle plate, row nail blocking, and spring plate for acetabular posterior column fractures involving the quadrilateral area of the acetabulum. The results suggest that there are no significant differences among the fixations.

Citation: Xie XJ, Cao SL, Tong K, Zhong ZY, Wang G. Three-dimensional finite element analysis with different internal fixation methods through the anterior approach. *World J Clin Cases* 2021; 9(8): 1814-1826

URL: <https://www.wjgnet.com/2307-8960/full/v9/i8/1814.htm>

DOI: <https://dx.doi.org/10.12998/wjcc.v9.i8.1814>

INTRODUCTION

With the modernization of society and transportation in the last several decades in China, the incidence of high-energy trauma, including acetabular fractures, has increased sharply in China^[1-3]. The life-time prevalence of hip fracture is 20% in women and 10% in men^[4], and acetabular fractures represent 18% of the total hip arthroplasty procedures in Chinese patients^[5]. In China from 2002 to 2006, the incidence of hip fractures increased 2.8- and 1.6-fold in women and men, respectively^[6]. The treatment of acetabular fracture is challenging. Presently, the primary treatment of displaced acetabular fracture is still open reduction and internal fixation^[4,7-11].

The fractures of the quadrilateral area of the acetabulum are not included in the Letournel classification^[12,13], but many complex fractures of the acetabular posterior column involve the quadrilateral area of the acetabulum^[14,15]. Although the load-bearing area of the acetabulum is mainly at its top, not at the quadrilateral area, when a high-energy injury occurs, the quadrilateral area as a part of the inner wall of the posterior column is often hit into the pelvis by the femoral head and displaced together with the posterior column^[15]. Moreover, anatomical reduction and fracture fixation aim to restore the matching relationship of the acetabulum and avoid leaving a central subluxation of the hip joint and traumatic arthritis, with a significant impact on clinical efficacy^[11,16,17]. Previous studies suggested using a 1/3 tubular steel plate or L-shaped steel plate to block the displacement of the acetabulum-related structures^[15,18,19]. Zha *et al*^[16] suggested using a multidirectional fixation device with pelvic brim long screws. Nevertheless, the preoperative planning of such fractures is complicated because of the complex anatomy of the hip.

In the traditional biomechanical studies of the pelvis, human cadavers are often used, but the measurements of displacement and stress in cadaver specimens inevitably lead to large errors. Cadaveric specimens have the disadvantages of high cost, limited availability, and difficulty in repeated tests. In addition, cadaveric

specimens will lead to systematic errors because even though the bones and joints retain their properties, the properties of the soft tissues will inevitably suffer from rigor mortis and the fixative/preservative solutions. In many studies, the soft tissues are removed, and only the bones and the joint are kept, but all information about the contribution of the tendons, fascia, and muscles to the stability of the joint is lost^[20,21]. Therefore, at present, three-dimensional (3D) finite element modeling is an effective method for biomechanical research^[22,23]. Nevertheless, in order to ensure the success of the experiment and the accuracy of the data, it is necessary to reconstruct the bone model accurately. The pelvis and acetabulum are a complex bony structure with cancellous bone sandwiched in the cortex^[24]. Because the muscles and ligaments around the acetabulum play an indispensable role in stabilizing the pelvis bone structure and reducing stress concentration^[25], it is necessary to pay attention to the addition of important ligaments when modeling to obtain a 3D finite element model of the pelvis with high simulation value and good stability.

At present, no biomechanical study has evaluated the stability of a 3D finite element model for the modeling of the treatment of acetabular posterior column fractures involving the quadrilateral area of the acetabulum. Therefore, the present study aimed to use a finite element model to establish different internal fixation models of the internal iliac plate, combined plate of anterior and posterior columns, triangle plate, row nail blocking, and spring plate and to simulate the standing and sitting positions. Using advanced mathematical modeling techniques, a mathematical model of an actual hip joint was obtained and could be used to measure forces, and stresses could be measured at specific points and under different conditions. The results will provide a basis for determining the biomechanical characteristics of the fixation of acetabular posterior column fractures.

MATERIALS AND METHODS

Finite element models of the pelvis

A 48-year-old healthy male volunteer was selected as the research subject. This individual had undergone a vasectomy and had no plans for fertility. The risks and possible harms were carefully explained, and he signed the informed consent form, which was first approved by the ethics committee along with the study protocol. His pelvis was scanned using a dual-source 16-row computed tomography scanner (Siemens, Erlangen, Germany). The bone tissue window was selected for scanning. The thickness of the scanning layers was 1.0 mm, and the scanning range was from the upper edge of the fifth lumbar vertebra to the upper part of the bilateral femur, including the whole ischial tubercle. The computed tomography images were imported into Mimics 17.0 (Materialise, Leuven, Belgium) to generate the 3D model of the pelvis. The .stl file saved from Mimics 17.0 was opened in Geomagic Studio 2013 (Geomagic Inc., Morrisville, NC, United States), and the model was subdivided by 4 × mesh to ensure that no serious deformation occurred during model processing. The accurate pelvis, sacrum, and femur models were obtained after removing the redundant deformation features of the model and the sharp nail-like objects. The precise surface module was used to detect the contour of the model, edit the deformed or unreasonable contours, add the contour appropriately, and generate more regular surface pieces to fit the surface model. Then, the geometry model was exported to the general Step format to build a 3D model of a normal pelvis.

Using SolidWorks 2014 (Dassault Systems SolidWorks Corporation, Waltham, MA, United States) and according to the software prompts, feature recognition and surface diagnosis of the geometric models were carried out, and the problematic surfaces were repaired. Then, the model was saved to the SLDPRT part format. After the vertebral body model was inserted in the way of origin matching and all cancellous bones were copied using the duplicated cancellous bone model as the subtractive entity, the Boolean operation was performed on the pelvis model to obtain the model of the complete pelvis cortical and cancellous bones. The upper and lower surfaces of each sacrum and pelvis cortical bone were treated equidistantly, and the equidistant distance was 0 mm. The sacroiliac joint cartilage was established between them. The redundant part of the equidistant surface was then excised to make it fit the sacrum and pelvis entirely. Similarly, the acetabulum cartilage on both sides was generated, and a completely normal 3D model was obtained. The above geometric model was imported into Ansys 17.0 (ANSYS Inc., Canonsburg, PA, United States), and the analysis type was specified as "Static Structural." Then, the property parameters of each material were set in the material library, as shown in [Table 1](#).

Table 1 Material property parameters of the main structures of the pelvis

Part	Modulus of elasticity in MPa	Poisson's ratio
Pubic cartilage	5.00	0.45
Interosseous sacroiliac ligament	5610.00	0.20
Sacrum	6140.00	0.30
Sacrospinous ligament	12.60	0.20
Sacrospinous ligament	46.48	0.300
Sacroiliac joint cartilage	54.00	0.40
Iliac cancellous bone	132.00	0.20
Femur	18200.00	0.38
Posterior sacroiliac ligament	133.00	0.20
Acetabular cartilage	12.00	0.42
Iliac cortical bone	17000.00	0.30
Anterior sacroiliac ligament	208.00	0.20

In the connection interface, the contact type between each structure was defined, in which the contact of the joint surface was set to “frictional,” and the corresponding friction coefficient was 0.5. The other contact types were set as “bonded,” which means that the relative position relationship of the structures on both sides of the contact surface was fixed. The spring element was used to simulate the ligament, and the tensile stiffness of each ligament was set. Next, the model was divided into meshes. In order to ensure the accuracy of the calculation to meet the requirements of the analysis, the type and size of the mesh were controlled. The mesh was set as the tetrahedral mesh with a size of 2 mm. Finally, the 3D finite element model of the pelvis was generated without error (Figure 1).

Fracture model

The right acetabular posterior column fracture model involving the quadrilateral area of the acetabulum was finally generated by setting up the reference plane, marking the fracture line, and cutting the fracture model according to the fracture line (Figure 2).

Surgical techniques

Using SolidWorks 2014 (Dassault Systems SolidWorks Corporation, Waltham, MA, United States), the models of the combined steel plate of anterior and posterior columns, internal iliac steel plate, row nail, triangle steel plate, and spring steel plate were generated by determining the equidistant surface, setting the datum plane and drawing the sketch of steel plate, drawing the boss, cutting with the tangent plane, cutting and stretching, and drawing the details of the steel plate. Then, they were imported into the 3D model of the pelvic posterior column fracture. Finally, different internal fixation models of the posterior acetabular column involving the quadrilateral area of the acetabulum were generated (Figure 3).

Loading and stress analyses

The upper surface of the sacrum was set as a rigid plane to simulate the sitting position and bipedal standing position under the human physiological state. The gravity of the upper half of the adult body was equivalent to a pressure of 600 N and uniformly loaded along the gravity axis. In the standing position, the lower end face of the femur was restrained, and the freedom of the six directions of the relevant nodes was set to zero to ensure that the plane composed of the bilateral anterior superior iliac spine and pubic symphysis was parallel to the gravity axis. Then, the stress and displacement distributions of the pelvis model in the standing position were calculated. In the sitting position, the bilateral ischial tubercle was restrained, and the freedom of the six directions of the relevant nodes was set to zero to ensure that the midpoint of the line between the lowest points of the bilateral ischial tubercles was perpendicular to the gravity axis. Then, the stress and displacement distributions of the pelvis model in the sitting position were calculated.

After the restraint and load were applied, ten points evenly distributed on the

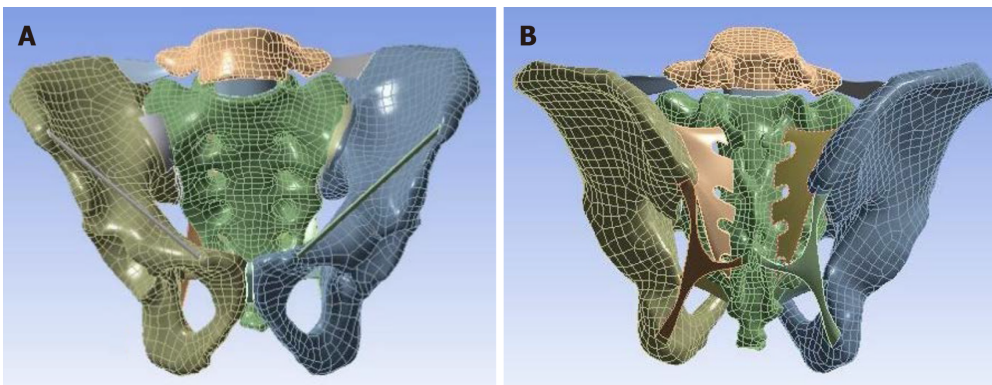


Figure 1 Finite element mesh of the pelvis model. A: Front view; B: Back view.

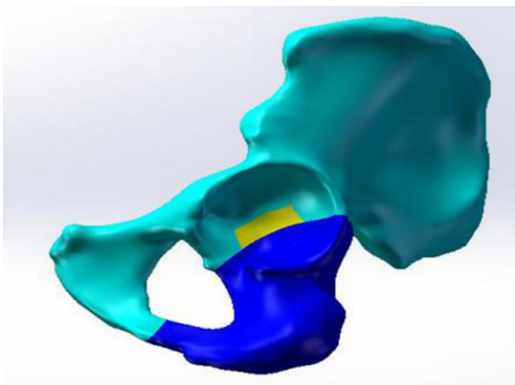


Figure 2 Establishment of the acetabular posterior column fracture model involving the quadrilateral area of the acetabulum.

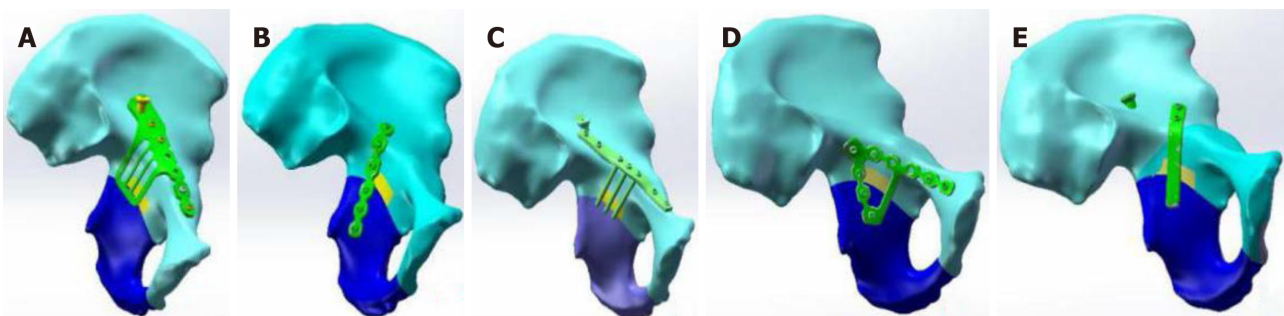


Figure 3 Different internal fixation models of acetabular posterior column fractures involving the quadrilateral area of the acetabulum. A: Combined plate of anterior and posterior columns; B: Internal iliac plate; C: Row nail; D: Triangle plate; E: Spring plate.

fracture line of the posterior column and quadrilateral area of the acetabulum in the acetabulum fossa were selected, and the stress and displacement data were measured in the sitting and standing positions. At the same time, the maximum stress and displacement of the ten points were obtained. Then, the displacement and stress distribution on the fracture line of the different internal fixation models were compared. In general, the more unstable the internal fixation, the greater the stress and displacement. The measurement indexes were: (1) The stiffness of the acetabulum structure was used to reflect the overall stability of the acetabulum after treatment of the fracture with different internal fixation; and (2) The stress distribution, the maximum value, and its position with different internal fixation methods were measured. According to the properties of the different materials, the mechanical characteristics were evaluated, and the possibility and location of failure of internal fixation were predicted.

Statistical analysis

Statistic Package for Social Science 22.0 (IBM Corp., Armonk, NY, United States) was used for statistical analysis. Continuous data conforming to the normal distribution (according to the Kolmogorov-Smirnov test) were presented as means \pm SD, while those not conforming to the normal distribution were presented as medians (range). The mean values of stress and displacement at each point were compared among fixations. For the variable not normally distributed, the Kruskal-Wallis test was used, followed by the Dunnett-*t* post hoc test. For the indexes with a normal distribution, one-way analysis of variance and the Bonferroni post hoc test were used. *P* values < 0.05 indicated statistical significance.

RESULTS

Validation of the pelvic model

Figure 4 presents the validation of the simulation of the biomechanical conduction process. As can be seen by the colors on the model (dark blue indicating the smallest relative stress/displacement and red the highest), in the standing position, the stress applied on the sacral endplate was transmitted to the bilateral sacroiliac joints and ilium through the sacrum, backward and downward through the posterior acetabular column, forward through the medial arcuate edge of the pelvis to the pubic symphysis, and finally to the bilateral lower limbs through the hip joint. The maximum stress was 46.210 MPa. In the sitting position, the stress distribution of the pelvis was from top to bottom, and the sacrum bore the simulated gravity load at the upper end, which has a downward and forward displacement trend. The stress was mainly concentrated in the sacroiliac joint, posterior column, superior ischial branch, and pubic branch. The specific measurement data are shown in [Supplementary Table 1](#).

Comparisons among stress distributions and displacements of the fragment lines

For the combined plate of the anterior and posterior columns in the sitting position, the stress on the fracture line was mainly concentrated in the middle of the acetabular fossa. The maximum stress was 2.296 MPa, the maximum displacement was 0.938 mm, and the average displacement was 0.604 ± 0.286 mm. In the standing position, the stress on the fracture line was mainly concentrated above the acetabulum. The maximum stress at each node of the fracture line was 1.880 MPa, the maximum displacement was 0.240 mm, and the average displacement was 0.140 ± 0.049 mm (Tables 2 and 3).

For the internal iliac plate in the sitting position, the stress on the fracture line of the left acetabulum was mainly concentrated in the anterior and superior acetabulum. The maximum stress at the fracture end was 2.653 MPa, the maximum displacement was 0.590 mm, and the average displacement was 0.444 ± 0.136 mm. In the standing position, the stress on the fracture line was mainly concentrated in the posterior and superior acetabulum. The maximum stress at each node of the fracture line was 1.815 MPa, the maximum displacement was 0.241 mm, and the average displacement was 0.146 ± 0.044 mm (Tables 2 and 3).

For the row nail blocking technology in the sitting position, the maximum stress at the fracture end of the left acetabulum was 2.726 MPa, the maximum displacement was 1.109 mm, and the average displacement was 0.694 ± 0.286 mm. In the standing position, the stress on the fracture line of the left acetabulum was mainly concentrated in the posterior and superior acetabulum. The maximum stress at each node of the fracture line was 2.683 MPa, the maximum displacement was 0.244 mm, and the average displacement was 0.150 ± 0.046 mm (Tables 2 and 3).

Regarding the triangle plate in the sitting position, the stress on the fracture line of the left acetabulum was mainly concentrated in the front and upper part of the joint. The maximum stress was 2.803 MPa, the maximum displacement was 0.914 mm, and the average displacement was 0.677 ± 0.227 mm. In the standing position, the stress on the fracture line of the left acetabulum was mainly concentrated in the upper part of the acetabulum. The maximum stress at each node of the fracture line was 2.507 MPa, the maximum displacement was 0.237 mm, and the average displacement was 0.147 ± 0.042 mm (Tables 2 and 3).

For the spring plate in the sitting position, the stress on the fracture line of the left acetabulum was mainly concentrated in the anterior part of the acetabulum. The maximum stress at the fracture end was 2.735 MPa, the maximum displacement was 1.125 mm, and the average displacement was 0.817 ± 0.283 mm. In the standing

Table 2 The stress of each point on the fracture line, in MPa

Node	Combined steel plate		Internal iliac plate		Row nail blocking		Triangular steel plate		Spring steel plate	
	Sitting	Standing	Sitting	Standing	Sitting	Standing	Sitting	Standing	Sitting	Standing
1	0.470	0.891	0.549	0.703	0.606	0.827	0.485	0.568	0.538	0.650
2	0.812	0.299	0.991	0.376	1.200	0.239	1.227	0.412	1.142	0.483
3	1.285	0.653	1.213	0.792	1.197	1.105	1.298	0.923	1.186	0.792
4	2.296	0.603	1.929	0.624	2.314	0.612	2.305	0.706	2.401	0.654
5	2.017	1.880	2.117	1.597	2.153	2.683	2.129	2.507	2.113	2.019
6	2.664	1.751	2.653	1.815	2.726	1.920	2.803	1.192	2.735	1.803
7	0.535	0.154	0.509	0.173	0.541	0.187	0.551	0.180	0.547	0.161
8	0.592	1.153	0.603	1.128	0.614	1.164	0.597	1.226	0.602	1.092
9	0.783	1.228	0.790	1.316	0.793	1.357	0.785	1.366	0.798	1.124
10	0.947	0.776	0.938	0.839	0.951	0.914	0.963	0.814	0.971	0.785
Mean	1.240	0.939	1.229	0.936	1.310	1.101	1.314	0.989	1.303	0.956
SD	0.757	0.541	0.708	0.497	0.756	0.719	0.778	0.618	0.772	0.547
Minimum value	0.470	0.154	0.509	0.173	0.541	0.187	0.485	0.180	0.538	0.161
Maximum value	2.296	1.880	2.653	1.815	2.726	2.683	2.803	2.507	2.735	2.019

In the sitting position, there were no statistical differences among groups ($P = 0.979$). In the standing position, there were no statistical differences among groups ($P = 0.974$). SD: Standard deviation.

position, the stress was mainly concentrated in the posterior and upper part of the acetabulum. The maximum stress at each node of the fracture line was 2.019 MPa, the maximum displacement was 0.257 mm, and the average displacement was 0.171 ± 0.042 mm (Tables 2 and 3).

When comparing the five fixations, the results showed no statistically significant differences in the mean values of stress among the groups (sitting position: $P = 0.9794$; standing position: $P = 0.9741$) (Table 2). In terms of displacement, there was a statistically significant difference among the groups in the sitting position ($P = 0.004$), and the pairwise comparisons showed that the average displacement of the internal iliac plate group was significantly smaller than that of the spring plate group ($P = 0.002$), and no differences were observed between the other pairs of groups (all $P > 0.05$). In the standing position, there were no significant differences in the mean value of displacement among the groups ($P = 0.2985$) (Table 3).

Stress distribution of the internal fixation methods

It can be seen from the stress nephogram of the internal fixations in different positions that the stress of the internal fixation was mainly concentrated in the fracture segment, indicating that the internal fixations had considerable stress on the fracture segment, and the possibility of internal fixation failure was relatively high in this part (Figure 5).

DISCUSSION

The standing and sitting positions are the most physiological postures in daily human life. Therefore, in this study the stability of the fixation of the acetabulum posterior column fracture involving the quadrilateral area of the acetabulum was analyzed with each internal fixator in the standing and sitting positions. The results suggest no significant differences among the fixations for the acetabular posterior column fracture involving the quadrilateral area of the acetabulum. The fixation effect of the spring plate was relatively poor.

Of course, the pressure load was different in the standing and sitting positions. Indeed, in the standing position, the stress applied on the sacral endplate was

Table 3 Displacement of each point on the fracture line, in mm

Node	Combined steel plate		Internal iliac plate		Row nail blocking		Triangular steel plate		Spring steel plate	
	Sitting	Standing	Sitting	Standing	Sitting	Standing	Sitting	Standing	Sitting	Standing
1	0.097	0.089	0.085	0.099	0.087	0.103	0.093	0.107	0.102	0.141
2	0.910	0.103	0.481	0.086	0.956	0.097	0.914	0.105	1.104	0.127
3	0.938	0.112	0.458	0.102	0.683	0.124	0.832	0.120	1.017	0.136
4	0.104	0.093	0.484	0.128	1.109	0.115	0.753	0.098	0.936	0.128
5	0.887	0.121	0.401	0.157	0.990	0.131	0.914	0.144	1.125	0.205
6	0.682	0.117	0.377	0.128	0.887	0.135	0.756	0.126	0.913	0.146
7	0.652	0.129	0.473	0.172	0.633	0.153	0.671	0.167	0.801	0.182
8	0.556	0.194	0.503	0.172	0.545	0.201	0.539	0.187	0.714	0.214
9	0.520	0.198	0.588	0.171	0.511	0.198	0.597	0.178	0.618	0.201
10	0.690	0.239	0.590	0.241	0.538	0.244	0.702	0.237	0.843	0.257
Mean	0.604	0.140	0.444	0.146	0.694	0.150	0.677	0.147	0.817	0.171
SD	0.286	0.049	0.136	0.044	0.286	0.046	0.227	0.042	0.283	0.042
Minimum value	0.097	0.089	0.085	0.086	0.087	0.097	0.093	0.098	0.102	0.127
Maximum value	0.938	0.240	0.590	0.241	1.109	0.244	0.914	0.237	1.125	0.257

In the sitting position, there was a statistical difference in the means among groups ($P = 0.004$). The pairwise comparisons indicated that the average displacement of the internal iliac plate group was significantly smaller than that of the spring plate group ($P = 0.002$). There were no other significant pairwise differences (all $P > 0.05$). In the standing position, there were no significant differences in the means among groups ($P = 0.299$). SD: Standard deviation.

transmitted to the bilateral sacroiliac joints and ilium through the sacrum, backward and downward through the posterior acetabular column, forward through the medial arcuate edge of the pelvis to the pubic symphysis, and finally to the bilateral lower limbs through the hip joint. In the sitting position, the stress distribution of the pelvis was from top to bottom, and the sacrum bore the simulated gravity load at the upper end, which had a downward and forward displacement trend. The stress was mainly concentrated in the sacroiliac joint, posterior column, superior ischial branch, and pubic branch. Those measurements were in concordance with what was expected from those positions as supported by previous studies^[22,26,27].

In this study, the spring plate fixation showed a worse effect than the other fixation methods. It might be because the distal end of the plate cannot be fixed with screws, and the displacement of the distal end cannot be controlled. If the steel plate is over shaped when the steel plate is placed, then the steel plate near the pelvic edge will not fit the bone surface. There were no significant differences among the combined plate, internal iliac plate, row nail blocking, and triangle plate fixation for acetabulum posterior column fracture involving the quadrilateral area of the acetabulum. Those results might suggest that those four fixation devices can be used interchangeably, but their specific application should be combined according to each patient's clinical and individual conditions.

Various studies used a finite element model to assess the impact of different fixation devices for hip fractures. Fan *et al*^[28] compared the double-column reconstruction plate, the anterior column plate combined with posterior column screws, and the anterior column plate combined with quadrilateral area screws in T-shaped acetabular fractures and showed that the anterior column plate combined with quadrilateral area screws achieved the best outcomes in terms of pressure and displacement. Using a similar approach, Lei *et al*^[29] compared the same three fixations except for hemitransverse acetabular fractures and showed that the anterior column plate combined with quadrilateral area screws also achieved the best outcomes. Yildirim *et al*^[30] suggested that anterior or posterior column screws were superior to two-column support for transverse acetabular fracture. The direct comparison of those three studies with the present one is difficult because of the differences in fracture

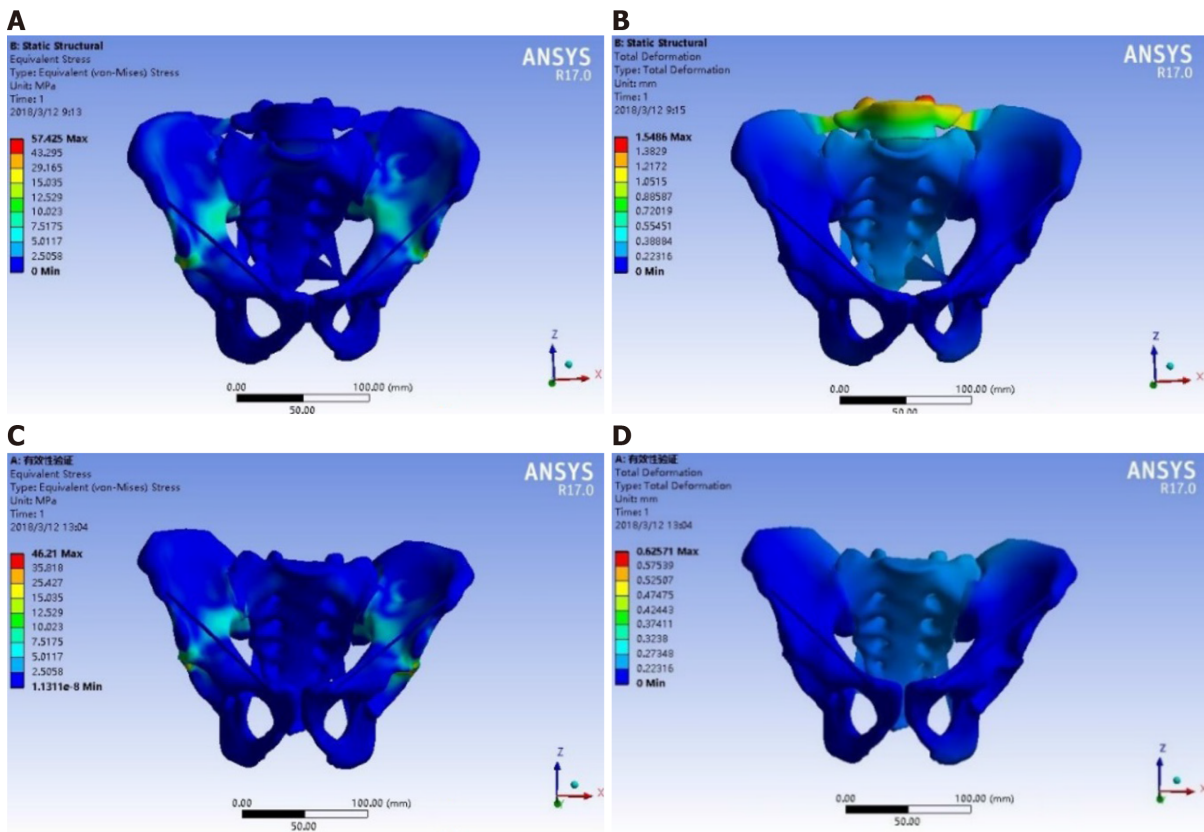


Figure 4 Stress distribution and displacement distribution of the pelvis in the standing and sitting positions. Dark blue indicates the smallest stress and displacement, while light blue, green, yellow, orange, and red indicate gradually higher stress and larger displacement. A: Stress distribution in the standing position; B: Displacement distribution in the standing position; C: Stress distribution in the sitting position; D: Displacement distribution in the sitting position.

types. Nevertheless, the present study suggests that the internal iliac plate resulted in the smallest displacement in the sitting position.

The present study has limitations. The finite element model has shortcomings. Because of the complex structure of the pelvis and acetabulum, the thickness of the cortical bone and the amount of cancellous bone are different between each bone block and different parts of the same bone block, and there are also differences between different individuals. Therefore, it is inevitable to observe errors compared with clinical practice when assigning an elastic modulus and Poisson’s ratio to a specific bone block. Second, in terms of a simplified model, this experiment includes the reconstruction of muscles and ligaments. When modeling, because of the use of the spring element to simulate a ligament, there is a large stress concentration on the surface of the cortical bone in the pelvis model, which has a certain error with the actual reality of the solid pelvis^[31]. In this study, it is assumed that the materials involved are continuous and homogeneous, which is not consistent with the characteristics of non-uniformity, heterogeneity, and nonlinearity found in actual human tissues. Due to the computing limitations, it is impossible to analyze every point on the fracture line, so there are some differences between the experimental results and reality. In addition, a fracture of the quadrilateral area of the acetabulum is often comminuted, which is challenging to simulate. Finally, the model was constructed from a single healthy volunteer. Because hip fractures are more frequent in elderly and osteoporotic women, future studies should also examine those patient types and make comparisons among them.

CONCLUSION

In conclusion, ten points on the fracture line of the posterior column and quadrilateral area of the acetabulum in the acetabulum fossa were measured for stress and displacement data in the sitting position and standing position using five different fixation devices. There were no significant differences among the fixations for the acetabular posterior column fracture involving the quadrilateral area of the

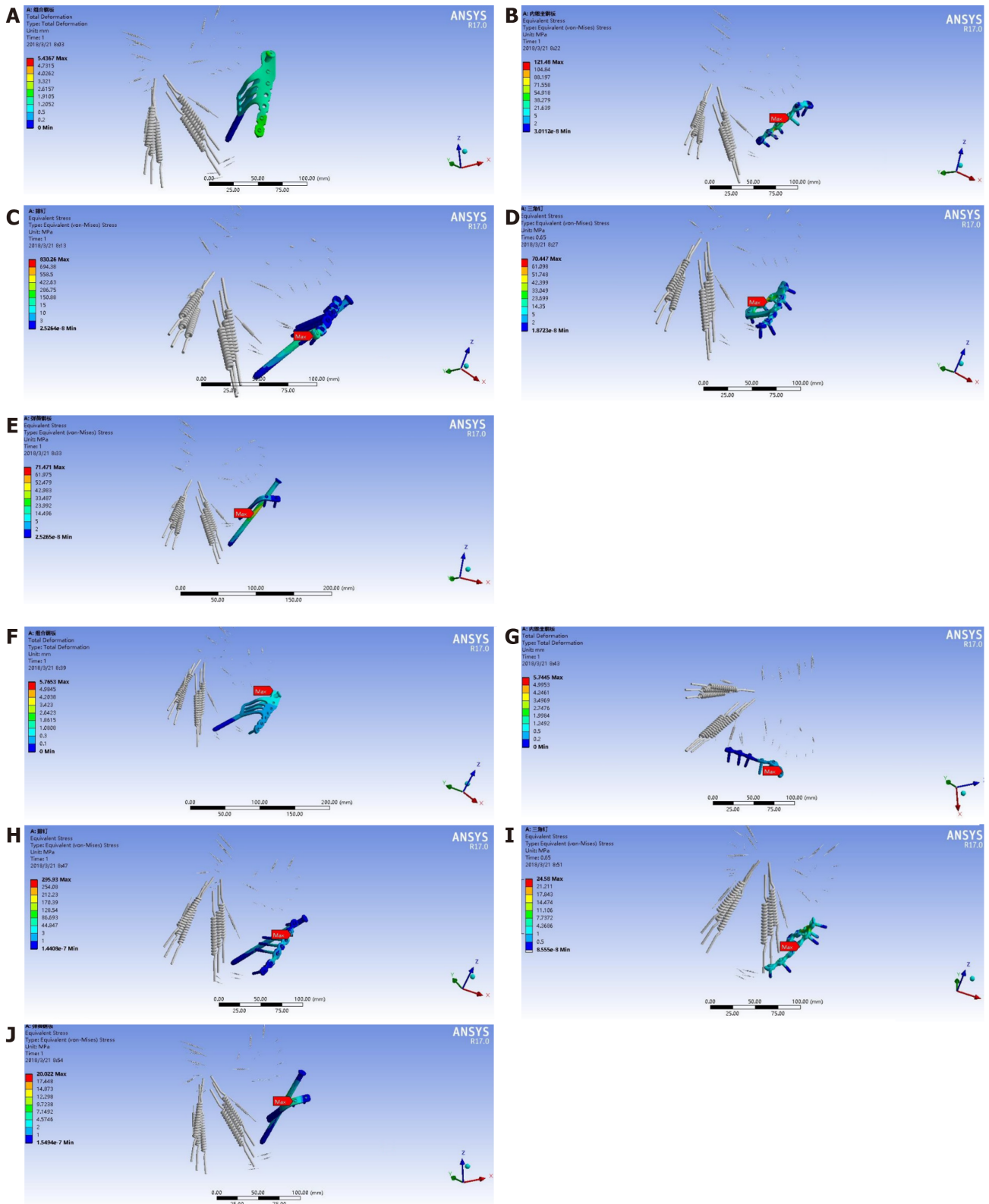


Figure 5 Stress distribution of different internal fixation. The grey parts represent the pelvis, and the materials in blue and green are the internal fixation devices. Dark blue indicates the smallest stress and displacement, while light blue, green, yellow, orange, and red indicate gradually higher stress. A-E: Sitting position; F-J: Standing position.

acetabulum. The fixation effect of the spring plate was relatively poor, while the internal iliac plate resulted in the smallest displacement in the sitting position. The results provide a basis for the biomechanical characteristics of acetabular posterior column fracture fixation.

ARTICLE HIGHLIGHTS

Research background

With the modernization of society and transportation in the last several decades in China, the incidence of high-energy trauma, including acetabular fractures, has increased sharply in China.

Research motivation

The treatment of acetabular fractures is challenging, especially for fractures of the quadrilateral area. Obtaining a three-dimensional finite element model of the pelvis is an effective method for biomechanical research and can provide a basis for the biomechanical characteristics of different fixation methods applied in acetabular posterior column fracture.

Research objectives

This study aimed to establish different finite element models (in simulated standing and sitting positions) of the internal iliac plate, combined plate of anterior and posterior columns, triangle plate, row nail blocking, and spring plate for acetabular posterior column fractures involving the quadrilateral area of the acetabulum.

Research methods

The three-dimensional models of the normal and fractured pelvis and the five internal fixations were established using computed tomography data of the pelvis of a living volunteer.

Research results

In the standing position, the maximum stress was 46.210 MPa. In the sitting position, the sacrum bore the simulated gravity load at the upper end. When comparing the five fixations, there were no significant differences in the stress mean values among groups. The average displacement of the internal iliac plate group was smaller than that of the spring plate group, and no differences were observed between the other pairs of groups. In the standing position, there were no significant differences in the mean value of displacement among the groups. Of note, the data were obtained from the model constructed from a single individual. The results should be validated in multiple individuals.

Research conclusions

There were no significant differences among the fixations for acetabular posterior column fractures involving the quadrilateral area of the acetabulum.

Research perspectives

The results provide a basis for the biomechanical characteristics of acetabular posterior column fracture fixation. Nevertheless, future studies should examine patients with different characteristics (*e.g.*, elderly, female, or osteoporotic) and patients with different types of fractures because simple posterior column fracture is not commonly seen, and this fracture model cannot satisfy the biomechanical studies of all kinds of posterior column fractures.

REFERENCES

- 1 **Stevens JA**, Rudd RA. The impact of decreasing U.S. hip fracture rates on future hip fracture estimates. *Osteoporos Int* 2013; **24**: 2725-2728 [PMID: 23632827 DOI: 10.1007/s00198-013-2375-9]
- 2 **Brauer CA**, Coca-Perraillon M, Cutler DM, Rosen AB. Incidence and mortality of hip fractures in the United States. *JAMA* 2009; **302**: 1573-1579 [PMID: 19826027 DOI: 10.1001/jama.2009.1462]
- 3 **Mauffrey C**, Hao J, Cuellar DO 3rd, Herbert B, Chen X, Liu B, Zhang Y, Smith W. The epidemiology and injury patterns of acetabular fractures: are the USA and China comparable? *Clin Orthop Relat Res* 2014; **472**: 3332-3337 [PMID: 24442842 DOI: 10.1007/s11999-014-3462-8]
- 4 **LeBlanc KE**, Muncie HL Jr, LeBlanc LL. Hip fracture: diagnosis, treatment, and secondary prevention. *Am Fam Physician* 2014; **89**: 945-951 [PMID: 25162161]
- 5 **Chung TC**, Chen TS, Hsu YC, Kao FC, Tu YK, Liu PH. Long-term total hip arthroplasty rates in patients with acetabular and pelvic fractures after surgery: A population-based cohort study. *PLoS One* 2020; **15**: e0231092 [PMID: 32243484 DOI: 10.1371/journal.pone.0231092]
- 6 **Xia WB**, He SL, Xu L, Liu AM, Jiang Y, Li M, Wang O, Xing XP, Sun Y, Cummings SR. Rapidly

- increasing rates of hip fracture in Beijing, China. *J Bone Miner Res* 2012; **27**: 125-129 [PMID: 21956596 DOI: 10.1002/jbmr.519]
- 7 **Peter RE.** Open reduction and internal fixation of osteoporotic acetabular fractures through the ilio-inguinal approach: use of buttress plates to control medial displacement of the quadrilateral surface. *Injury* 2015; **46** Suppl 1: S2-S7 [PMID: 26528936 DOI: 10.1016/S0020-1383(15)70003-3]
 - 8 **Florschutz AV,** Langford JR, Haidukewych GJ, Koval KJ. Femoral neck fractures: current management. *J Orthop Trauma* 2015; **29**: 121-129 [PMID: 25635363 DOI: 10.1097/BOT.0000000000000291]
 - 9 **Sagi HC,** Afsari A, Dziadosz D. The anterior intra-pelvic (modified rives-stoppa) approach for fixation of acetabular fractures. *J Orthop Trauma* 2010; **24**: 263-270 [PMID: 20418730 DOI: 10.1097/BOT.0b013e3181dd0b84]
 - 10 **Hirvensalo E,** Lindahl J, Böstman O. A new approach to the internal fixation of unstable pelvic fractures. *Clin Orthop Relat Res* 1993; 28-32 [PMID: 8242945 DOI: 10.1097/00003086-199312000-00007]
 - 11 **Farid YR.** Cerclage wire-plate composite for fixation of quadrilateral plate fractures of the acetabulum: a checkrein and pulley technique. *J Orthop Trauma* 2010; **24**: 323-328 [PMID: 20418739 DOI: 10.1097/BOT.0b013e3181e90bbe]
 - 12 **Tile M.** Fractures of the pelvis and acetabulum. 2nd ed. Baltimore: Williams & Wilkins, 1995
 - 13 **Judet R,** Judet J, Letournel E. Fractures of The Acetabulum: Classification and Surgical Approaches For Open Reduction. Preliminary Report. *J Bone Joint Surg Am* 1964; **46**: 1615-1646 [PMID: 14239854 DOI: 10.2106/00004623-196446080-00001]
 - 14 **Scheinfeld MH,** Dym AA, Spektor M, Avery LL, Dym RJ, Amanatullah DF. Acetabular fractures: what radiologists should know and how 3D CT scan aid classification. *Radiographics* 2015; **35**: 555-577 [PMID: 25763739 DOI: 10.1148/rg.352140098]
 - 15 **Wu YD,** Cai XH, Liu XM, Zhang HX. Biomechanical analysis of the acetabular buttress-plate: are complex acetabular fractures in the quadrilateral area stable after treatment with anterior construct plate-1/3 tube buttress plate fixation? *Clinics (Sao Paulo)* 2013; **68**: 1028-1033 [PMID: 23917670 DOI: 10.6061/clinics/2013(07)22]
 - 16 **Zha GC,** Sun JY, Dong SJ, Zhang W, Luo ZP. A novel fixation system for acetabular quadrilateral plate fracture: a comparative biomechanical study. *Biomed Res Int* 2015; **2015**: 391032 [PMID: 25802849 DOI: 10.1155/2015/391032]
 - 17 **Douraiswami B,** Vinayak G. Isolated Quadrilateral Plate Fracture of the Acetabulum - a unique case Scenario. *J Orthop Case Rep* 2012; **2**: 32-34 [PMID: 27298851]
 - 18 **Laflamme GY,** Hebert-Davies J, Rouleau D, Benoit B, Leduc S. Internal fixation of osteopenic acetabular fractures involving the quadrilateral plate. *Injury* 2011; **42**: 1130-1134 [PMID: 21156315 DOI: 10.1016/j.injury.2010.11.060]
 - 19 **Qureshi AA,** Archdeacon MT, Jenkins MA, Infante A, DiPasquale T, Bolhofner BR. Infrapectineal plating for acetabular fractures: a technical adjunct to internal fixation. *J Orthop Trauma* 2004; **18**: 175-178 [PMID: 15091273 DOI: 10.1097/00005131-200403000-00009]
 - 20 **Losco M,** Familiari F, Giron F, Papalia R. Use and Effectiveness of the Cadaver-Lab in Orthopaedic and Traumatology Education: An Italian Survey. *Joints* 2017; **5**: 197-201 [PMID: 29270555 DOI: 10.1055/s-0037-1608949]
 - 21 **Matuszewski S,** Hall MJR, Moreau G, Schoenly KG, Tarone AM, Villet MH. Pigs vs people: the use of pigs as analogues for humans in forensic entomology and taphonomy research. *Int J Legal Med* 2020; **134**: 793-810 [PMID: 31209558 DOI: 10.1007/s00414-019-02074-5]
 - 22 **Zhang L,** Peng Y, Du C, Tang P. Biomechanical study of four kinds of percutaneous screw fixation in two types of unilateral sacroiliac joint dislocation: a finite element analysis. *Injury* 2014; **45**: 2055-2059 [PMID: 25457345 DOI: 10.1016/j.injury.2014.10.052]
 - 23 **Wako Y,** Nakamura J, Matsuura Y, Suzuki T, Hagiwara S, Miura M, Kawarai Y, Sugano M, Nawata K, Yoshino K, Orita S, Inage K, Ohtori S. Finite element analysis of the femoral diaphysis of fresh-frozen cadavers with computed tomography and mechanical testing. *J Orthop Surg Res* 2018; **13**: 192 [PMID: 30064512 DOI: 10.1186/s13018-018-0898-7]
 - 24 **Jacob HA,** Huggler AH, Dietschi C, Schreiber A. Mechanical function of subchondral bone as experimentally determined on the acetabulum of the human pelvis. *J Biomech* 1976; **9**: 625-627 [PMID: 965413 DOI: 10.1016/0021-9290(76)90103-2]
 - 25 **Lin SQ,** Wang B, Zhang L, Yang CJ. Application and research progress of finite element analysis in orthopaedics. *Zhongguo Zhongyi Gushangke Zazhi* 2013; **21**: 69-73 [DOI: CNKI:SUN:ZGZG.0.2013-04-035]
 - 26 **Li Z,** Kim JE, Davidson JS, Etheridge BS, Alonso JE, Eberhardt AW. Biomechanical response of the pubic symphysis in lateral pelvic impacts: a finite element study. *J Biomech* 2007; **40**: 2758-2766 [PMID: 17399721 DOI: 10.1016/j.jbiomech.2007.01.023]
 - 27 **Anderson AE,** Peters CL, Tuttle BD, Weiss JA. Subject-specific finite element model of the pelvis: development, validation and sensitivity studies. *J Biomech Eng* 2005; **127**: 364-373 [PMID: 16060343 DOI: 10.1115/1.1894148]
 - 28 **Fan Y,** Lei J, Zhu F, Li Z, Chen W, Liu X. Biomechanical Analysis of the Fixation System for T-Shaped Acetabular Fracture. *Comput Math Methods Med* 2015; **2015**: 370631 [PMID: 26495030 DOI: 10.1155/2015/370631]
 - 29 **Lei J,** Dong P, Li Z, Zhu F, Wang Z, Cai X. Biomechanical analysis of the fixation systems for anterior column and posterior hemi-transverse acetabular fractures. *Acta Orthop Traumatol Turc*

- 2017; **51**: 248-253 [PMID: 28342586 DOI: 10.1016/j.aott.2017.02.003]
- 30 **Yildirim AO**, Alemdaroglu KB, Yuksel HY, Öken ÖF, Ucaner A. Finite element analysis of the stability of transverse acetabular fractures in standing and sitting positions by different fixation options. *Injury* 2015; **46** Suppl 2: S29-S35 [PMID: 26028425 DOI: 10.1016/j.injury.2015.05.029]
- 31 **Phillips AT**, Pankaj P, Howie CR, Usmani AS, Simpson AH. Finite element modelling of the pelvis: inclusion of muscular and ligamentous boundary conditions. *Med Eng Phys* 2007; **29**: 739-748 [PMID: 17035063 DOI: 10.1016/j.medengphy.2006.08.010]



Published by **Baishideng Publishing Group Inc**
7041 Koll Center Parkway, Suite 160, Pleasanton, CA 94566, USA
Telephone: +1-925-3991568
E-mail: bpgoffice@wjgnet.com
Help Desk: <https://www.f6publishing.com/helpdesk>
<https://www.wjgnet.com>

